Age-depth relationship and associated uncertainty of englacial radar layers in Marie Byrd Land, West Antarctica

Gail Gutowski, Charles Jackson, Duncan Young, Donald Blankenship
Institute for Geophysics, University of Texas at Austin

December 4, 2015

Abstract

We present estimates of the age-depth relationship for ten radar reflectors in the Marie Byrd Land sector of West Antarctica, near the WAIS Divide and Byrd ice core sites. We compute a range of ages for these radar reflectors which incorporate uncertainties from radar and ice core measurements. An ice flow model is used to simulate the depth dependence of layers. The Metropolis-Hastings algorithm is used to invert for ice flow parameters which lead to age-depth profiles consistent with observations to within uncertainty.

We present ten layers that have been traced and dated in this region to a depth of **X** m. We find age-depth uncertainty introduced by radar is approximately 2 m and is constant with depth below 168 m. Combined with an assumed 3% uncertainty in age in the ice column from ice core dating, we find that some pairs of spatially distinct radar horizons are consistent with being isochronous deposition events. This information is useful in determining the duration of past events affecting ice fabric, such as volcanic eruptions, which deposit dust with a prominent dielectric contrast in the ice column. Ambiguities in the age-depth relationship also suggests the importance of including a complete accounting of uncertainty, including chronologic uncertainty, to fully describe the dynamic evolution of the ice sheet.

1 Introduction

Ice sheet response to changes in climatic conditions in the past can be useful for anticipating the response of the existing West Antarctic Ice Sheet (WAIS) to current global warming. The Thwaites Glacier catchment in Marie Byrd Land is of particular interest because it is thinning in response to modern climate change and may further destabilize in the future citation. Understanding the past dynamics of the WAIS during similar climates could inform estimates of current WAIS stability and predictions of future WAIS flow.

Age-depth profiles are one tool to reveal ice dynamics and accumulation history by exploring the distribution of ice age as a function of depth. In recent years, ice-penetrating radar has made it possible to extend one-dimensional age-depth profiles measured at ice cores over hundreds of kilometers in the West Antarctic Ice Sheet [e.g. *Neumann et al.*, 2008; *Holt et al.*, 2006]. This allows for englacial layer dating over an extensive three-dimensional region of the ice sheet.

Ice-penetrating radar, like ice cores, provide a window into the depths of the ice sheet where a record of the past ice sheet is preserved. Using remote-sensing radar systems, it is possible to efficiently collect this spatially extensive englacial layer information. It is possible to assign dates to the radar-detected englacial layers by also collecting radar near ice cores with measured chronologies. Layer geometry can then be used to investigate WAIS flow during past climate regimes.

Errors arise in both radar-derived layer depths and ice core age profiles. Such errors become larger at greater depths, where strain thinning and complex past flow hampers interpretation of the ice core chronology and layer identification. It is necessary to account for these sources of uncertainty when mapping dates to englacial radar layers. To quantify the age-depth uncertainty from these measurement errors, we use a Bayesian method to compute a range of physically reasonable age-depth profiles. Each profile in the ensemble also honors the physical dependence of layer ages in the ice column using a simple ice flow model. The resulting ensemble of profiles represent an envelope of age-depth estimates which agree with observations to within depth and age uncertainty for a series of prominent radar reflectors.

2 Data

2.1 Radar Data

Several surveys have acquired ice-penetrating radar-echo sounding (RES) data of the WAIS, including Airborne Geophysical Survey of the Amundsen Sea Embayment [AGASEA *Holt et al.*, 2006], Geophysical Investigations of Marie Byrd Land Evolution [GIMBLE **?**], and others [e.g. **??**]. The data includes two-way travel times (TWTT; the time it takes for a radar pulse to be transmitted, reflect off an englacial layer, and return to the receiver) in microseconds collected using a 60 MHz center frequency. GIMBLE data was collected with the High Capacity Airborne Radar Sounder (HiCARS) system. HICARS uses a 1 s chirp width with a 15 MHz bandwidth corresponding to a 100 ns pulse width after compression (?8.4 m in ice) and a 6.4 kHz pulse repetition frequency (PRF). Signals were digitized at 20 ns intervals and coherently stacked ten times, log detected and incoherently stacked five times to yield records every ?22 m along-track (Young and others, 2011). We also use ice-penetrating radar colllected by the CReSIS Multi-Channel Coherent Radar Depth Sounder (MCoRDS) [**?**]. The MCoRDS system operates in a frequency range between 180 MHz and 210 MHz. It uses multiple receivers and an adjustable bandwidth up to 30 MHz. This leads to 4.5 m vertical resolution in ice and 30 m along-track sampling [**?**].

Ten radar layers were traced through radargrams from these surveys using the seismic imaging softwares *GeoFrame* and *LandMark's* Decision Space Desktop based on peaks and troughs in processed signal amplitude. These softwares employ semi-automated tracking algorithms to track peaks in return signal using an adjustable travel-time window. The layers were selected for their prominent signal and continuity through the MBL domain. Crossovers between RES flight lines allowed for extensive layer tracking. Tracked layers may end where discontinuities or waning signal prevented reliable tracing. The layers included are shown in Figure 1 in a radargram of an ice sheet cross section near the WAIS Divide ice core.

2.2 WAIS Divide ice core chronology

The WAIS Divide ice core (see Figure **??**; 79.48°S, 112.11°W), is the most recent to be drilled in Antarctica [**?**]. Annual layer counting to 2850 m depth and methane synchronization to 3404 m depth were used to determine a

chronology for the ice core. The core reached 50 m above the estimated bed depth to avoid contaminating the basal hydrology system. The oldest ice in the core has been dated to 68ka at high resolution (0.5 m to 2m at depth). High resolution and precision are achievable at the WAIS Divide site because of high accumulation rate and methane synchronization method used to determine the deep chronology.

2.3 Byrd ice core chronology

The Byrd ice core (see Figure **??**;), drilled in 1968, was the first in Antarctica to extend to bedrock [*Gow et al.*, 1968]. Damage to the ice core above 88 m prohibited the traditional approach of annual layer counting. However, a shallow core drilled nearby in 1989 (NBY89) enabled *Langway et al.* [1994] to complete a chronology for the top 164 m of the ice column. Below 88 m, the electrical conductivity method (ECM) was used to date the ice core [*Hammer et al.*, 1994]. The ECM method measures variations in electrical conductivity. Between 300 m and 900 m, brittle ice precluded sufficient ECM measurements, so *Hammer et al.* [1994] instead fit the chronology with three piecewise linear functions. The resulting layer-thickness profile was integrated from surface to depth to obtain an age-depth relationship for the length of the ice core.

Hammer et al. [1997] present a volcanic chronology of the Byrd ice core based on this previously-derived timescale in which volcanic events were matched to peaks in electrical conductivity, consistent with the presence of ash in the ice column. The chronology includes dated volcanic events between 709 BP and more than 18,000 BP, corresponding to depths ranging from 97.8 m to 1890 m below the 1968 surface of the Byrd ice core. We use part of this volcanic record to 1358 m depth (corresponding to 20594 a) as an observational constraint on our age-depth profile.

3 Sources of Uncertainty

3.1 Radar Depth Estimates and Uncertainty

Radar-acquired TWTT is converted to layer depth beneath the ice surface using constant electromagnetic (EM) velocities in ice and air (168.5 m/μs and 300 m/μs, respectively). These velocities are derived using a dielectric

constant in ice of $\epsilon^{'} = 3.17$ [*Peters et al.*, 2005; **?**] and the common relation $C_{ice} = C_{air}/\sqrt{\epsilon^{'}}$. Firn corrections are applied to the depth of each layer, according to the *Dowdeswell* [2004] relation:

$$z_f = \frac{K}{n_i^{'}} \int (\rho_i - \rho(z))dz \tag{1}$$

where K is 0.85 m^3Mg^{-1} [**?**], $n_i^{'}$ is the refractive index of ice (1.78), ρ_i is the density of ice (0.917 Mg m^{-3}) and $\rho(z)$ is the density of ice at depth z with units Mg m$^-$3.

Two sources contribute to errors in the computed layer depths: 1) vertical resolution limitations due to digitized pulse width sampling effects and 2) variations in EM wave propagation in ice, both due to density variations in the firn layer and due to variations in ice fabric and temperature.

Vertical resolution varies based on each radar system's measured radar pulse width [**?**]. The finite pulse width means that an infinitesimally thin layer of ice will appear in the survey to have a finite width. The error in phase sampling of this pulse is typically $\frac{\lambda}{2}$, but can be as accurate as $\frac{\lambda}{4}$ for data with high signal-to-noise (λ is the wavelength of the electromagnetic pulse). The sampling rate for the data used here varies from 5 ns to 20 ns. Conservatively, we assume a 10 ns resolution when tracking the phase of layer detections. We then randomly sample from a normal distribution with mean 0 and standard deviation (10 ns) for the HiCARS radar system, which was used to determine the age-depth profile at each ice core.

Errors in the firn correction are computed from the error in density profiles measured at each ice core . Ice density data as a function of depth were obtained from the original analysis of the ice core [*Gow et al.*, 1968]. The data were used to account for the varying density of ice and subsequent variations in electromagnetic wave speed through the firn layer at the top of the ice sheet. EM velocity in ice varies from 168 to 169.5 $m/\mu s$ [**?**], leading to increasing uncertainty with depth. Again assuming these errors are normal, we independently randomly sample each error from a normal distribution with mean 0 and standard deviation equivalent to the quoted depth error above.

It is important to note that the computed depth of each layer is relative to the ice surface as also measured by the HiCARS radar. While each layer may have errors independent of the others, errors in the distance of the surface from the acquisition aircraft are systematic across all observed

layers. Therefore, a randomly sampled error due to the vertical resolution is computed for the surface and the same error is applied to all radar layers. Additionally, all layers of interest lie below the computed firn layer at each ice core site. The firn correction error is therefore also systematically applied to all subsequent radar layers.

To compute the total uncertainty in depth to each layer, we take the RMS of the surface error, firn correction error, and EM propagation error (independently sampled for each of the ten layers of interest). Uncertainty increases with depth, as expected and is approximately .

3.2 Age Estimates and Uncertainty

We interpret the englacial layers as isochronous under the assumption that each continuous layer of ice sharing dielectric properties was deposited at the surface at same time [*Eisen et al.*, 2004]. Estimates of the age of ice throughout each ice core is completed using isotopic analysis, such as methane synchronization [**?**] and the electrical conductivity method [*Hammer et al.*, 1997]. Absolute dates are obtained by correlating the Antarctic ice cores with absolute records from the Greenland Ice Sheet such as the GRIP ice core. Absolute dating is also possible using correlation with known and dated global volcanic events.

Estimates of errors in dating the WAIS Divide ice core are approximate and according to expert opinion. We expect larger age errors in ice deeper where shear thinning results in layers that are more difficult to distinguish from one another and where disruptions in shallower parts of the ice core can contribute error to dating deeper layers. We assume errors are 3% of the ice age, which is on the conservative end of expert opinion (personal communication T.J. Fudge, 2013). Without additional information for uncertainty analysis, we contend this is an appropriate first-order description of the age errors.

The ice core chronology at Byrd is uncertain due to damage in the upper part of the core, a zone of brittle ice between 788 m and 900 m depth, subjectivity in the interpretation of ECM results, among other reasons. *Hammer et al.* [1994] suggest a precision of $\pm$ 1000 years for 20 ka ice due to subjectivity in the ECM technique. They also give an approximate accuracy of 1 ka ice as $\pm$ 500 years. The volcanic chronology developed by *Hammer et al.* [1997] quotes $\pm$ 500 years for the prominent Old Faithful radar horizon observed to be approximately 17400 a old. Due to a lack of uncertainty analysis of the

ice core chronology, we assume an uncertainty distribution that is 3% of the observed age of the ice column, the same assumed for the WAIS Divide ice core. For example, this assumes that Old Faithful is of age 17400 ± 522 a and that a layer of age 10 ka has uncertainty ± 300 years.

4 Method

The depth-age profile is determined at both the WAIS Divide and Byrd ice cores as a check on the calculation. The ten layers selected for this study are observed near both ice cores and can be directly tracked continuously between the two. As a result, the age of each layer determined at the two ice cores sites should be consistent to within uncertainty.

Different ice flow models were used for the WAIS Divide and Byrd ice cores because of differences in their position on the ice sheet. The ice flow physics at an ice sheet divide are more straightforward because the velocity of ice is primarily vertical. Ice flow off the divide, such as near the Byrd ice core, can be more complex. The two ice flow models are described below.

4.1 WAIS Divide ice core flow model

4.2 Byrd ice core flow model

At the Byrd ice core site, we use an ice flow model derived for conditions at the Byrd ice core by *Morland* [2009] to determine the age of internal layers near the Byrd ice core drilling site in Antarctica. The model has the form:

$$\begin{aligned} \frac{\overline{z}}{h_0} &= \frac{1}{1-r}[1 - exp(-s\bar{t})] \\ \overline{z} &= h_0 - z \\ r &= \frac{b}{q} \\ s &= s_d s_0 \end{aligned} \tag{2}$$

where depth, $\overline{z}$, is defined to be 0 at the base, $h_0 = 2164$ m is the depth at the ice sheet surface, b is basal melting rate, q is the accumulation rate, and $\bar{t}$ is the age corresponding to $\overline{z}$. The optimum constant strain rate, s, is used to achieve reasonable correlations between the model and observations; s_0 is the initial strain rate and s_d is determined empirically for the Byrd ice core to be $s_d = 0.722$ for the Byrd ice core [*Morland*, 2009]. The model assumes isostatic equilibrium, constant ice density, uniform strain rate in z, and $r < 1$ (i.e. nonnegative mass balance in the ice column). Further, while depth in the model, $\overline{z}$, is defined so that $\overline{z}$(base) $= 0$, the following analysis is discussed in terms of depth z, where *z(surface)* $= 0$.

Note that it is difficult to know accumulation rate on its own due to layer thinning at depth within the ice column. As such, we consider layer thickness instead of layer accumulation because it can be physically measured using the techniques described previously. We use a stepwise function to parameterize accumulation in four depth regimes:

$$z = \begin{cases} z_1 & \text{z} < 150\text{m} \\ z_2 & 150\text{m} \leq \text{z} < 1024m \text{ m} \\ z_3 & 1024\text{m} \leq \text{z} < 1294\text{m} \\ z_4 & \text{z} \geq 1292\text{m} \end{cases}$$

These regimes were chosen based on a linear piecewise function of layer thickness developed by *Hammer et al.* [1994] in which slope changes are observed at the above transition points. We use the flow model to invert for accumulation as a function of depth, q, and strain scale factor, s, [*Morland*, 2009, see] using an observed age-depth relationship.

We use the resulting parameters to evaluate the age of the ten radar layers of interest. The inversion is done using a Markov Chain Monte Carlo technique known as the Metropolis-Hastings algorithm *Metropolis et al.* [1953].

4.3 MCMC inversion

We are interested in finding appropriate flow model parameters which lead to age-depth profiles consistent with the observational data. To do so, the flow models are inverted for the parameters described above. Acceptable parameter values are those which describe flow consistent with the observed age-depth relationship at the ice core sites.

The Metropolis-Hastings algorithm utilizes prior knowledge about the model parameters for each model to develop a joint posterior distribution of

the parameters. We use truncated uniform priors on all parameters, allowing them to take on values within a physically reasonable range, as described in the preceding sections. The model is initialized using random parameter values within these ranges.

At each model step, we evaluate the age determined by the flow model at every point in the ice column based on proposed sets of parameters. An associated likelihood is evaluated as a measure of the model-data misfit for each proposal. The log likelihood is described in equation 3:

$$log(likelihood) = \frac{(Age_{model} - Age_{obs})^2}{(2\sigma_{obs})^2} \tag{3}$$

where Age_{model} comes from evaluating the ice flow model for an ice core site given proposed parameters. Age_{obs} and σ_{obs} come from from the WAIS Divide ice core chronology and the volcanic age-depth function for the Byrd ice core, respectively. We allow for the uncertainty in Age_{obs} (σ_{obs}) to loosen the constraint on how closely the Age_{model} must match Age_{obs} to be acceptable.

At each iteration, the algorithm makes a decision about whether or not to accept the combination of parameters based on the likelihood function, which may also beknown as the cost function. If the cost of the nth iteration is less than the cost of the *(n-1)*th iteration, the set of parameters is accepted. This means that the nth set of parameters is a better fit to the data, because the cost has decreased. If the cost has not decreased, there is still a chance the algorithm will accept the parameter set. This enables a full exploration of parameter space in the event there are multiple modes in the posterior. If the cost of the nth iteration is greater than the cost of the *(n-1)*th iteration, the set of parameters is accepted with probability $exp[-\frac{cost_n - cost_{n-1}}{2}]$, the Metropolis probability. After each evaluation of the cost function, the algorithm continues on a random walk through parameter space for a pre-determined number of iterations.

We use the Metropolis algorithm to generate a large number of age-depth distributions that together describe the probability of the age of a radar layer based on knowledge about ice flow and the layer's depth. We generate 20,000 sets of flow parameters for each ice core site that characterize physically reasonable models of age-depth. Sampled age uncertainty is taken to be the standard deviation in age at a given depth.

4.4 Sampling radar depth uncertainty

Uncertainty in the radar-derived depth of each layer is considered next. To find the radar sampling rate uncertainties, we randomly sample from the probability distribution for the surface reflector, described by σ_{surf}. We then randomly sample ten values from a probability distribution described by σ_{lay}, resulting in a radar sampling rate for each of the layers of interest. Total depth uncertainty for each radar horizon is taken to be the root mean square of sampling rate and EM wave propagation errors. This process is repeated 20,000 times to build a probability distribution describing the depth of each radar layer.

4.5 Determining the posterior distribution for age-depth relationship

Forward modeling is used to combine uncertainties in both age and depth into a distribution for the age-depth relationship. For each of the 20,000 iterations performed in the previous sections, we randomly select a depth sample and an age sample, each containing information for the full set of radar layers. The age-depth profile for each iteration is taken to be the evaluated ice flow model age for each sampled depth given the sampled flow parameters. The result is an ensemble of 20,000 age-depth profiles for the radar horizons of interest. Both depth and age to each radar layer may vary between ensemble members.

5 Results

Figure 2a shows the distribution of modeled depths associated with each layer of interest near the Byrd ice core site. The spread in the distribution is indicative of observational uncertainty. Table **??** shows the standard deviation in depth for each of the ten layers, assuming the errors are gaussian. See Section 3.2 for a full discussion of the sources of error included in this analysis. The uncertainty in each layer depth does not increase appreciably with depth. This indicates surface and firn uncertainties dominate.

The corresponding age distributions are shown in Figure 2b and again assume gaussian errors. Table **??** shows the mean and standard deviation for each layer's age distribution. Due to increased uncertainty in ice core

dating methods, age uncertainty increases with depth. As Figure 2 shows, layers at 738.8 ± 2.3 m and 759.1 ± 2.3 m (layers 7 and 8) are consistent within age uncertainty, indicating they may have been from the same snow deposition event. Similarly, layers 9 and 10 (1257.7 ± 2.4 m and 1266.2 ± 2.3 m depth) are barely distinct in depth, but are likely isochronous when age uncertainty is included in the analysis. This ambiguity makes it clear robust uncertainty quantification is critical for the interpretation of englacial layer chronology; dynamic analyses assume radar layers are from distinguishable events when obtaining a time-dependent profile of ice flow.

Figure 3 shows the ensemble of modeled age-depth distributions for the ten radar layers. The distributions are trained on the observed records from each ice core, allowing for uncertainties in both depth and age. Spread between estimate age-depth in the various ensemble members is representative of uncertainty in both age and depth measurements. As expected, uncertainties increase with depth and age uncertainty dominates depth uncertainty.

As described in Section 4, the Byrd ice core flow model is based on five parameters: layer thickness parameters in four depth regimes and a ratio of surface to bed ice velocity. Figure 5 shows the distributions of the layer thickness parameters, which are used as a proxy for accumulation in the model. As expected due to layer thinning with depth, mean layer thickness decreases deeper in the ice sheet. The modeled layer thickness is consistent with that at the Western Divide above 1294 m determined by [*Neumann et al.*, 2008]; Table **??** shows a comparison between the two. We expect layer thickness to be at a maximum at the divide and therefore reasonable values at Byrd Station should be less than those at the divide. Our modeled layer thickness below 1294 m is larger than shallower modeled thicknesses and greatly exceeds the layer thickness at the divide at this depth. However, this depth corresponds to only the deepest radar horizon of interest, so it should not affect the result.

6 Discussion

Our approach employs simple ice flow models applicable to each ice core site with additional basic assumptions. To further simplify the model used at the Byrd ice core site [*Morland*, 2009], we assume no basal melting, for example. This is a poor assumption for this location because liquid water was observed at the base of the ice sheet when the core was drilled to bedrock

[*Gow et al.*, 1968]. Geothermal flux derived from a borehole temperature profile was estimated to be 75 mW m^{-}2 by *Gow et al.* [1968], appreciable enough to induce ice melting at depth. Additionally, the model assumes only vertical strain, ignoring potentially important longitudinal contributions to ice flow. Ice near Byrd Station is flowing at $v_{surf} \sim 11$ m/a, about 0.5 km since the Byrd ice core was drilled, so it is important to include horizontal components in future analyses [*Bindschadler et al.*, 1997]. The large surveys of continuous radar observations make radar an ideal method for studying these kinds of longitudinal effects, which will be included with more complex models of ice flow in the future.

Future work should also look to improve upon the ice flow parameters and priors used in the MCMC inversion we applied. For example, these ice flow models rely heavily on the assumed function of ice accumulation. We use layer thickness as a proxy for accumulation at the Byrd ice core and assume a paleoclimate-inspired functional form for paleo accumulation at the WAIS Divide ice core. The sensitivity of these choices on the resulting age-depth distribution should be thoroughly tested against alternative assumptions.

While we thoroughly account for source of error in the vertical determination of age and depth, we do not consider errors in the longitudinal tracking of radar layers. As discussed more thoroughly below, errors introduced by human interpretation of the processed radar data via the seismic interpretation software must be considered quantitatively. This is possible by having multiple people independently reproduce the interpretation of layer depth throughout the domain and computing the differences between independent interpretations. Each individual's layer interpretation should form a closed loop in the domain, such that the depth of any layer interpreted near an ice core can be confirmed by an intersecting RES line.

This approach is sufficient for this study, wherein the age-depth profile is validated at only two points on the ice sheet, near the WAIS Divide and Byrd ice core sites. The extension away from the ice cores of the age-depth profile information derived here must include the same reproducibility and RES crossover analysis throughout the domain. Layer depth must be consistent at all crossover points to within the depth measurement error. Assuming layers are isochronous, the age uncertainty found for each layer should not vary based on position on the ice sheet.

7 Conclusion

We extend age-depth profiles derived from ice core records to the central WAIS using spatially extensive airborne RES survey data. The two are linked through simple ice flow models evaluated near ice core sites. This reveals dynamical information about past ice flow of the WAIS, important to paleoclimate studies and prediction of WAIS stability.

We include both systematic and random sources of uncertainty in evaluating the posterior distribution of the age-depth relationship at each ice core. Where age-depth profile samples cross (see Figure 3) indicate random uncertainty plays a significant part in the age-depth distribution of the ice layers at that site. Spread between ensemble members that do not cross is representative of systematic uncertainties in the model.

Our analysis reveals that when uncertainty is accounted for, radar layers which appear distinct in the ice column may be from the same ice deposition event. This result is important for the interpretation of past snow deposition. It may also reveal more significant human error in tracing radar layers through the domain. Figure 1 shows the vertical separation of ten radar layers used in this analysis. Layers 9 and 10 are vertically coincident for most of the domain shown, intuitively indicating the two are related depositional events. However, the two layers separate vertically in how they are traced at the point in the domain where this study focuses. This could be a real deformation in the ice due to flow or change in accumulation rate, but is likely an error in interpreting the vertical position of the layer in the geophysical software used to trace layers. Cases such as this will need to be evaluated on an individual basis. While outside errors such as those from the layer tracking software may persist, our method allows us to determine that despite increased layer thickness and therefore vertical separation between horizons 9 and 10 at our study's location, ice at the two horizons is consistent with having been deposited at the same time.

Importantly, the method described here preserves the dependence of layer depth within the ice column. While errors are considered independent for each layer, the age of layers in an ice column are not independent; deeper layers must be older than shallower layers. (An exception can be found in extreme cases of layer folding, but this is not observed in West Antarctica.) It is therefore necessary to use an ice flow model to construct age-depth profiles. A posterior distribution of age-depth profiles for the full column (as opposed to a posterior distribution of age determined independently at

each layer) is the most appropriate method of constraining the depositional information about each layer.

References

Bindschadler, R., X. Chen, and P. Vornberger, Surface velocity and strain rates at the onset of ice stream d, west antarctica, *Antarctic Journal of the United States*, *32*(5), 41–43, 1997.

Dowdeswell, J., Investigations of the form and flow of ice sheets and glaciers using radio-echo sounding, *Reports on Progress in Physics*, 2004.

Eisen, O., U. Nixdorf, F. Wilhelms, and H. Miller, Age estimates of isochronous reflection horizons by combining ice core, survey, and synthetic radar data, *Journal of Geophysical Research (Solid Earth)*, *109*, B04106, doi:10.1029/2003JB002858, 2004.

Gow, A. J., H. T. Ueda, and D. E. Garfield, Antarctic Ice Sheet: Preliminary Results of First Core Hole to Bedrock, *Science*, *161*, 1011–1013, doi:10.1126/science.161.3845.1011, 1968.

Hammer, C., H. Clausen, and C. Langway, 50,000 years of recorded global volcanism, *Climatic Change*, *35*(1), 1–15, 1997.

Hammer, C. U., H. B. Clausen, and C. C. Langway, Jr., Electrical conductivity method (ECM) stratigraphic dating of the Byrd Station ice core, Antarctica, *Annals of Glaciology*, *20*, 115–120, 1994.

Holt, J. W., D. D. Blankenship, D. L. Morse, D. A. Young, M. E. Peters, S. D. Kempf, T. G. Richter, D. G. Vaughan, and H. F. J. Corr, New boundary conditions for the West Antarctic Ice Sheet: Subglacial topography of the Thwaites and Smith glacier catchments, *Geophysical Research Letters*, *33*, L09502, doi:10.1029/2005GL025561, 2006.

Langway, C. C., Jr., K. Osada, H. B. Clausen, C. U. Hammer, H. Shoji, and A. Mitani, New chemical stratigraphy over the last millennium for Byrd Station, Antarctica, *Tellus Series B Chemical and Physical Meteorology B*, *46*, 40, doi:10.1034/j.1600-0889.1994.00004.x, 1994.

Depth Range (m)	Layer thickness at Divide (m)	Median Layer thickness at Byrd (m)
$d < 150$	~ 0.27	0.16 ± 0.04
$150 < d < 1024$	~ 0.14 - 0.27	0.13 ± 0.06
$1024 < d < 1294$	~ 0.08 - 0.14	0.10 ± 0.04

Table 1: Comparison between layer thickness at the Western Divide between the Ross and Amundson Seas [*Neumann et al.*, 2008] and modeled here at Byrd Station. Maximum layer thickness occurs at the divide, so layer thicknesses at Byrd Station are expected to be less, but comparable, at Byrd Station. We find that layer thickness at Byrd is the same as layer thickness at the Divide to within uncertainty, implying that our model is overestimating layer thickness. This is especially the case at depth, where we expect layer thinning to decrease the thickness of deeper layers due to increased strain. Uncertainties shown are at the 2σ level.

Metropolis, N., A. W. Rosenbluth, M. N. Rosenbluth, A. H. Teller, and E. Teller, Equation of state calculations by fast computing machines, *The Journal of Chemical Physics*, *21*(6), 1087–1092, doi: http://dx.doi.org/10.1063/1.1699114, 1953.

Morland, L. W., Age-depth correlation, grain growth and dislocation-density evolution, for three ice cores, *Journal of Glaciology*, *55*, 345–352, doi: 10.3189/002214309788608723, 2009.

Neumann, T. A., H. Conway, S. F. Price, E. D. Waddington, G. A. Catania, and D. L. Morse, Holocene accumulation and ice sheet dynamics in central West Antarctica, *Journal of Geophysical Research (Earth Surface)*, *113*, F02018, doi:10.1029/2007JF000764, 2008.

Peters, M. E., D. D. Blankenship, and D. L. Morse, Analysis techniques for coherent airborne radar sounding: Application to West Antarctic ice streams, *Journal of Geophysical Research (Solid Earth)*, *110*, B06303, doi: 10.1029/2004JB003222, 2005.

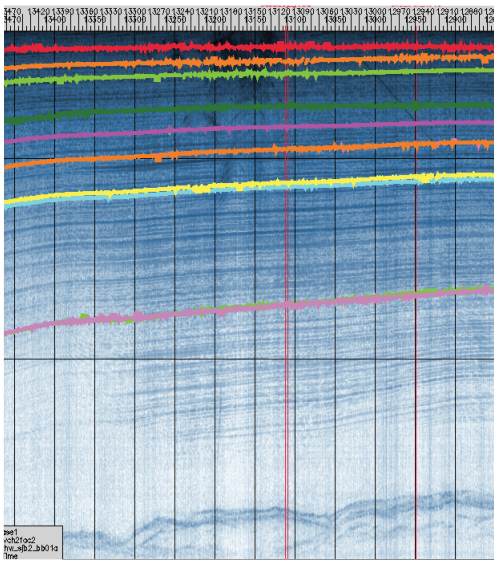

Figure 1: **a)** Spatial extent of 10 englacial horizons tracked through the WAIS for this study. **b)** Radargram of the area observed near Byrd ice core highlighting the ten radar horizons analyzed. The arrow on top of the figure indicates the location of the horizontal position of radar observations used. Our analysis shows that Horizons 7 and 8 and Horizons 9 and 10 are consistent within uncertainty to belonging to the same isochrone, though they appear distinct in the radargram. This emphasizes the importance of uncertainty quantification in interpretation of these horizons.

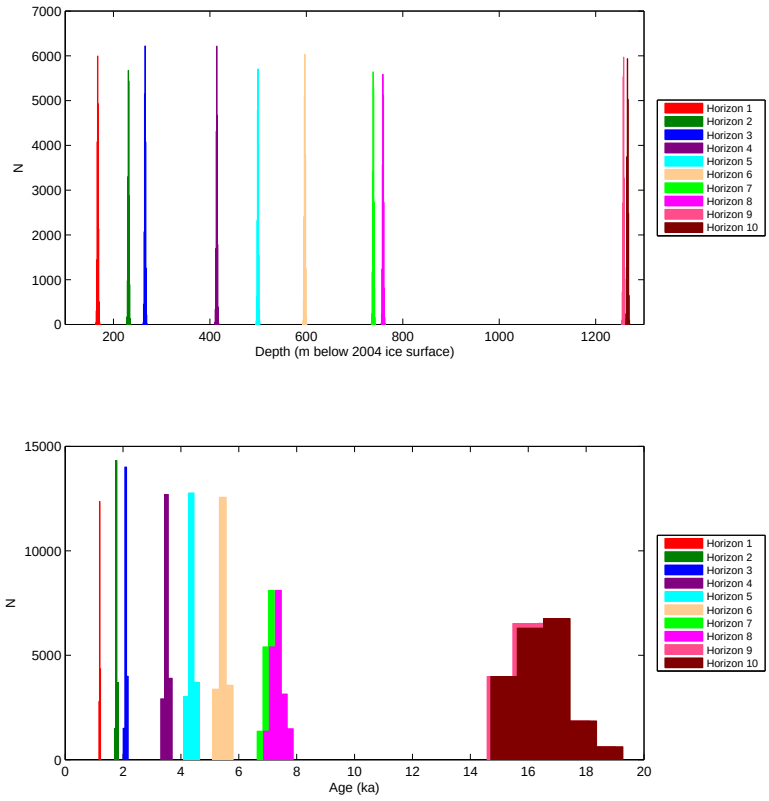

Figure 2: a) Histogram of modeled water-equivalent ice depth for each of ten prominent radar horizons observed using airborne radar near Byrd Station, West Antarctica. The width of each distribution is the result of uncertainties arising from the method of radar collection. b) Similar histogram in terms of age (ka). Age uncertainty comes from approximate uncertainty in ice core dating techniques.

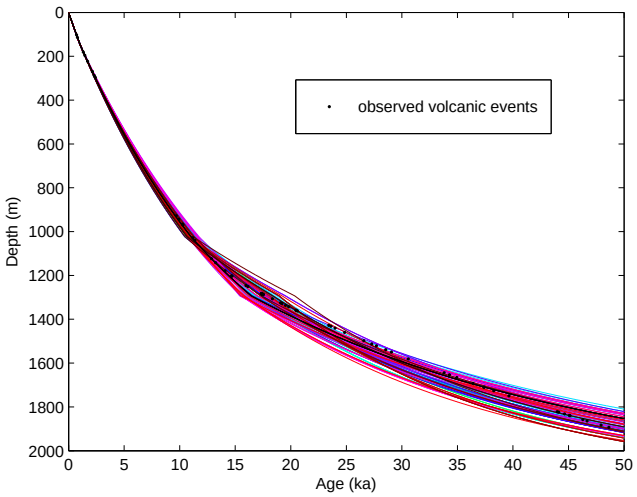

Figure 3: Ensemble of modeled age-depth profiles near Byrd ice core. Black dots represent dated volcanic events from the Byrd ice core record [*Hammer et al.*, 1994]. Each line represents a set of parameters that describe the observed data within uncertainty. (See Section 4.)

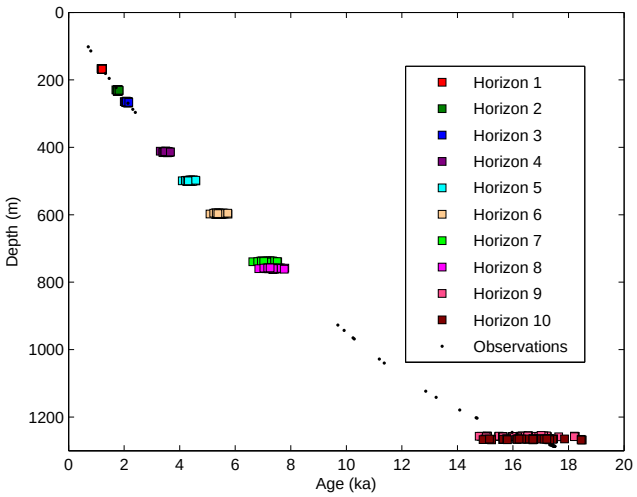

Figure 4: Age-depth profile of ten prominent radar horizons compared to an observed volcanic age-depth profile of the Byrd ice core. The depth and age of each radar horizon are randomly sampled within uncertainty to obtain an ensemble of possible values for that horizon.

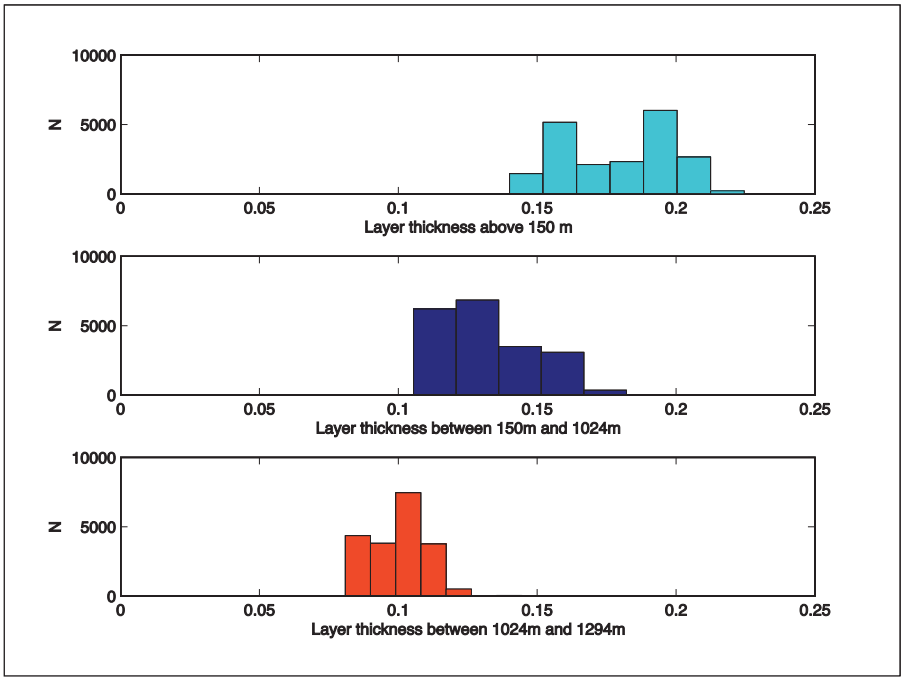

Figure 5: Modeled layer thickness in each of four depth regimes near Byrd Station, West Antarctica. The model overestimates layer thickness, particularly in deeper regimes.

Horizon	TWTT (μs)	Depth (m)			Age (a)		
		Mean	Median	σ	Mean	Median	σ
1	6.02	167.6	167.6	2.4	1200	1200	20
2	6.78	231.4	231.4	2.4	1770	1770	40
3	7.18	265.6	265.6	2.3	2100	2100	60
4	8.94	414.4	414.4	2.4	3510	3500	150
5	9.94	499.6	499.6	2.4	4360	4360	200
6	11.10	596.9	596.9	2.3	5440	5440	270
7	12.78	738.8	738.8	2.3	7120	7110	370
8	13.02	759.1	759.1	2.3	7350	7340	390
9	18.92	1257.7	1257.7	2.4	16220	16300	1760
10	19.02	1266.2	1266.2	2.3	16400	16500	1820

Table 2: Depth and age mean, median, and uncertainty for ten strong radar reflectors near Byrd Station, West Antarctica. The radar two-way travel time (TWTT) is given in column 1.